

Detecting Bose-Einstein condensation of exciton-polaritons via electron transport

Yueh-Nan Chen,^{1,*} Neill Lambert,² and Franco Nori^{2,3}

¹*Department of Physics and National Center for Theoretical Sciences, National Cheng-Kung University, Tainan 701, Taiwan*

²*Advanced Science Institute, The Institute of Physical and Chemical Research (RIKEN), Saitama 351-0198, Japan*

³*Physics Department and Center for Theoretical Physics, The University of Michigan, Ann Arbor, Michigan 48109-1040, USA*
(Received 12 August 2009; revised manuscript received 13 November 2009; published 30 December 2009)

We examine the Bose-Einstein condensation of exciton-polaritons in a semiconductor microcavity via an electrical current. We propose that by embedding a quantum dot *p-i-n* junction inside the cavity, the tunneling current through the device can reveal features of condensation due to a one-to-one correspondence of the photons to the condensate polaritons. Such a device can also be used to observe the phase interference of the order parameters from two condensates.

DOI: 10.1103/PhysRevB.80.235335

PACS number(s): 03.75.Nt

I. INTRODUCTION

The essence of Bose-Einstein condensation (BEC) is the macroscopic occupation of a single-particle state.^{1,2} The achievement of BEC in dilute atomic gases has enabled the study of the long-range spatial coherence in a well-controlled environment.² In contrast to the extremely low temperatures needed for dilute atom gases, excitons in semiconductors have long been considered a candidate for BEC at temperatures of a few Kelvin, due to their light effective mass.³ In the past few decades, numerous studies have shown evidence⁴ for the existence of excitonic BEC. A recent promising realization for such a BEC is within a two-dimensional quantum well in a microcavity, i.e., a condensate of polaritons,⁵ which are half-light, half-matter bosonic quasiparticles. Fascinating features of condensate polaritons, such as phase interference,⁶ quantized vortices,⁷ Bogoliubov excitations,⁸ and collective fluid dynamics,⁹ have been successfully observed in experiments.

In a context related to the study of semiconductor microcavities, an exciton in a quantum dot (QD) embedded inside a microcavity can be used to study the phenomena of cavity quantum electrodynamics.¹⁰ With the advances of fabrication and measuring technologies, strong couplings between the QD excitons and cavity photons have been observed both in a semiconductor microcavity¹¹ and in a photonic crystal nanocavity.¹² Another unique feature of artificial atoms, such as QDs, is that they can be connected to electronic reservoirs. For example, it is now possible to embed QDs inside a *p-i-n* structure,¹³ such that electrons and holes can be injected separately from opposite sides. This allows one to examine the exciton dynamics in a QD via electrical currents.¹⁴

Motivated by these recent developments, we propose a method to detect the BEC of polaritons via an electrical current by embedding a QD *p-i-n* junction inside a microcavity, where the condensation of polaritons takes place. This is, in principle, feasible since the excitation energy of the QD exciton (two-level spacing) is comparable to that of the cavity photons. Once the condensation of polaritons occurs, the one-to-one correspondence between the polariton and its half-light part (photon) ensures that the photons also condense to their ground state. In this case, the transport current through the dot should “feel” the condensation. We will

show that the contribution to the *coherent* transport of the current increases with the condensate fraction. Furthermore, if the QD is coupled to two condensates, the current-noise can reveal the phase interference between them.

II. QUANTUM DOT *p-i-n* JUNCTION IN A MICROCAVITY

Consider now a QD *p-i-n* junction embedded inside a semiconductor microcavity, where the quantum well excitons and cavity photons condense to their ground state as shown in Fig. 1(a). When this condensation occurs, a great number of polaritons, $\hat{b}_{\mathbf{k}}$, will occupy the zero-momentum state \mathbf{k}_0 . The canonical transformation^{1,2}

$$\hat{b}_{\mathbf{k}} = \sqrt{N'} e^{i\phi} \delta_{\mathbf{k}, \mathbf{k}_0} + \hat{a}_{\mathbf{k}} \quad (1)$$

is commonly used to describe N' condensed particles and noncondensate particles with operator $\hat{a}_{\mathbf{k}}$. The polariton operator $\hat{b}_{\mathbf{k}}$ is composed of the exciton operator, $\hat{c}_{\mathbf{k}}$, and photon operator, $\hat{a}_{\mathbf{k}}$,

$$\hat{b}_{\mathbf{k}} = u_{\mathbf{k}} \hat{c}_{\mathbf{k}} + v_{\mathbf{k}} \hat{a}_{\mathbf{k}}, \quad (2)$$

where $u_{\mathbf{k}}$ and $v_{\mathbf{k}}$ are coefficients easily obtained from the diagonalization of exciton-photon interaction.¹⁵ From Eq. (2), we can see that there is a one-to-one correspondence of the polariton operator to the photon one. Therefore, the canonical transformation in Eq. (1) can also be applied to the photon operator

$$\hat{a}_{\mathbf{k}} = \sqrt{N} e^{i\varphi} \delta_{\mathbf{k}, \mathbf{k}_0} + \hat{\beta}_{\mathbf{k}},$$

where $\hat{\beta}_{\mathbf{k}}$ represents the noncondensate photons. The photon condensate fraction N is related to N' via the particular choice of the diagonalization in Eq. (2).

Considering spinless fermions and neglecting the polarization of the photon, the exciton-photon interaction in the QD *p-i-n* junction, $H_{\text{ex-ph}}$, can now be written as

$$H_{\text{ex-ph}} = T_0 e^{i\varphi} |\uparrow\rangle\langle\downarrow| + \sum_{\mathbf{k}} D_{\mathbf{k}} |\uparrow\rangle\langle\downarrow| \hat{\beta}_{\mathbf{k}} + \text{H.c.}, \quad (3)$$

where $T_0 = \sqrt{N} D_{\mathbf{k}_0}$, with $D_{\mathbf{k}}$ being the coupling strength between the dot exciton and the cavity photon.

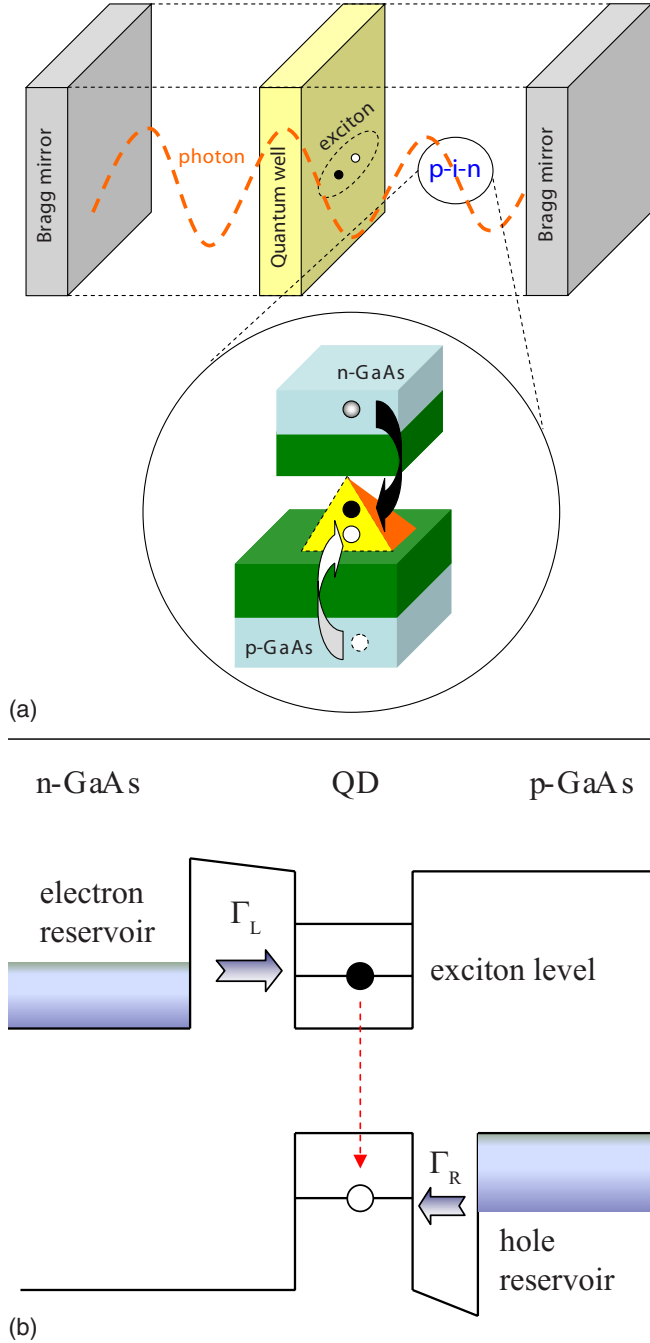


FIG. 1. (Color online) (a) Schematic diagram of the system: a semiconductor quantum well is placed between two Bragg mirrors. A quantum dot *p-i-n* junction is embedded between the well and the mirror to detect the photon part of the polaritons. For simplicity, the substrate of the QDs is not shown. (b) Energy-band diagram of a QD inside a *p-i-n* junction. The Fermi energy of the hole reservoir is aligned with the hole-level of the dot. After a hole tunnels into the dot, an electron can tunnel into the ground-state exciton level, with which the Fermi energy of the electron reservoir is aligned.

Here, we have assumed the photon energy to be on resonance with the QD (ground-state) exciton energy, i.e., the detuning is zero. In addition, the three dot states are introduced in Eq. (3): $|0\rangle=|0,h\rangle$, $|\uparrow\rangle=|e,h\rangle$, and $|\downarrow\rangle=|0,0\rangle$, where $|0,h\rangle$ means that there is one hole in the QD, $|e,h\rangle$ is

the exciton state, and $|0,0\rangle$ represents the ground state with no hole and no electron in the QD.¹⁴

One might argue that one cannot neglect the state $|e,0\rangle$ for real devices. This can be resolved by fabricating a thicker barrier on the electron side so that there is little chance for an electron to tunnel in advance. Also, the absence of bi-exciton and trion states can be justified by the following reasons: first, the Fermi energy of the hole reservoir is aligned with the hole level of the dot as shown in Fig. 1(b). After a hole tunnels into the dot, an electron can tunnel into the ground-state exciton level, with which the Fermi energy of the electron reservoir is aligned. Second, since we have assumed the photon energy to be on resonance with the QD (ground-state) exciton energy, the effect from other tunneling channels should be small and can be neglected in principle.

We have essentially assumed a mean-field interaction, so that the field of the condensate mode is just represented by a *c* number: there is no back action from the QD to the cavity. From the theory of transport through QDs, the first term in Eq. (3) represents *coherent* tunneling,¹⁶ while the second term describes *incoherent* tunneling.¹⁴ The Hamiltonian describing the tunneling to the electron and hole reservoirs can thus be written as

$$H_T = \sum_{\mathbf{q}} (V_{\mathbf{q}} \hat{d}_{e,\mathbf{q}}^\dagger |0\rangle\langle\uparrow| + W_{\mathbf{q}} \hat{d}_{h,\mathbf{q}}^\dagger |0\rangle\langle\downarrow| + \text{H.c.}), \quad (4)$$

where $\hat{d}_{e,\mathbf{q}}$ and $\hat{d}_{h,\mathbf{q}}$ are the electron operators in the electron and hole reservoirs, respectively. Here, $V_{\mathbf{q}}$ and $W_{\mathbf{q}}$ couple the channel with momentum \mathbf{q} of the electron and the hole reservoirs.

One can now write the equation of motion for the reduced density operator

$$\begin{aligned} \frac{d}{dt} \rho(t) = & -i[H_{\text{coh}}(t), \rho(t)] - \text{Tr}_{\text{res}} \int_0^t dt' \{H_{\text{incoh}}(t) \\ & + H_T(t), [H_{\text{incoh}}(t') + H_T(t'), \tilde{\Xi}(t')]\}, \end{aligned} \quad (5)$$

where $\tilde{\Xi}(t')$ is the total density operator, and H_{coh} (H_{incoh}) represents the coherent (incoherent) tunneling in Eq. (3). Note that the trace, Tr, in Eq. (5) is taken with respect to both the noncondensate photons and the electronic reservoirs.

III. TUNNELING CURRENT

If the couplings to the noncondensate photons and to the electron/hole reservoirs are weak, then it is reasonable to assume that the standard Born-Markov approximation with respect to these couplings is valid. In this case, one can derive the equations of motions of the system

$$\begin{aligned} \frac{\partial}{\partial t} \langle \hat{n}_{\uparrow} \rangle_t = & -iT_0(\langle \hat{p} \rangle_t - \langle \hat{p}^\dagger \rangle_t) - \gamma \langle \hat{n}_{\uparrow} \rangle_t \\ & + \Gamma_L(1 - \langle \hat{n}_{\uparrow} \rangle_t - \langle \hat{n}_{\downarrow} \rangle_t), \end{aligned}$$

$$\frac{\partial}{\partial t} \langle \hat{n}_{\downarrow} \rangle_t = iT_0(\langle \hat{p} \rangle_t - \langle \hat{p}^\dagger \rangle_t) + \gamma \langle \hat{n}_{\uparrow} \rangle_t - \Gamma_R \langle \hat{n}_{\downarrow} \rangle_t,$$

$$\begin{aligned}
\langle \hat{p} \rangle_t &= -iT_0 \int_0^t dt' e^{iE_0(t-t')} (\langle \hat{n}_\uparrow \rangle_{t'} - \langle \hat{n}_\downarrow \rangle_{t'}) \\
&\quad - \Gamma_R \int_0^t dt' e^{iE_0(t-t')} \langle \hat{p} \rangle_{t'}, \\
\langle \hat{p}^\dagger \rangle_t &= iT_0 \int_0^t dt' e^{-iE_0(t-t')} (\langle \hat{n}_\uparrow \rangle_{t'} - \langle \hat{n}_\downarrow \rangle_{t'}) \\
&\quad - \Gamma_R \int_0^t dt' e^{-iE_0(t-t')} \langle \hat{p}^\dagger \rangle_{t'}, \quad (6)
\end{aligned}$$

where $\hat{n}_\uparrow = |\uparrow\rangle\langle\uparrow|$, $\hat{n}_\downarrow = |\downarrow\rangle\langle\downarrow|$, $\hat{p} = |\uparrow\rangle\langle\downarrow|$, and $\hat{p}^\dagger = |\downarrow\rangle\langle\uparrow|$. Here, E_0 is the quantum dot exciton bandgap, Γ_L (Γ_R) is the tunneling rate from the electron-side (hole-side) reservoir, and γ is the incoherent decay rate due to the noncondensate photons. One can then obtain the tunnel current through the hole-side barrier:¹⁴ $I(t) \equiv -e\Gamma_R \langle \hat{n}_\downarrow \rangle_t$.

In the steady-state limit ($t \rightarrow \infty$), the analytical expression for the tunneling current I is given by

$$I(t \rightarrow \infty) = \frac{2\Gamma_R T_0^2 + 2\gamma\varepsilon^2}{[\varepsilon^2 + T_0^2(2 + \Gamma_R/\Gamma_L)] + \gamma\varepsilon^2(1/\Gamma_R + 1/\Gamma_L)}, \quad (7)$$

where $\varepsilon^2 = E_0^2 + \Gamma_R^2$. Note that, for convenience, we have set the electron charge $e=1$ and Planck constant $\hbar=1$. Examining Eq. (7) we note that, when the condensation number $N(\propto T_0^2)$ becomes relatively large, the steady-state current $I(t \rightarrow \infty)$ saturates to the value

$$I(t \rightarrow \infty) \rightarrow \frac{\Gamma_R}{N \rightarrow \infty} \frac{1}{1 + \frac{\Gamma_R}{2\Gamma_L}}, \quad (8)$$

depending only on the values of the tunneling rates Γ_L and Γ_R . In the opposite limit of no condensation, Eq. (7) is reduced to the result of incoherent case¹⁷

$$I(t \rightarrow \infty) \rightarrow \left(\frac{1}{\Gamma_R} + \frac{1}{\Gamma_L} + \frac{1}{\gamma} \right)^{-1}. \quad (9)$$

The curve in the inset of Fig. 2 shows that the current I increases when increasing the occupation number N . Such a phenomenon may be observed by increasing the power of the laser excitation, as has been performed in experiments.⁵ Note that in the inset of Fig. 2 and the following figures, we have set the exciton bandgap $E_0=1.4$ eV and the tunneling rates: $\Gamma_R=0.1$, $\Gamma_L=0.01$ meV.

IV. INTERFERENCE BETWEEN TWO CONDENSATES

Another important effect that can be examined is the interference between two condensates, which has been observed and verified in dilute atomic gases.¹⁸ Consider now an additional quantum well in the microcavity, so that the excitons in this well also form a condensate with the photons. The interactions experienced by the p - i - n junction experiences can be described by

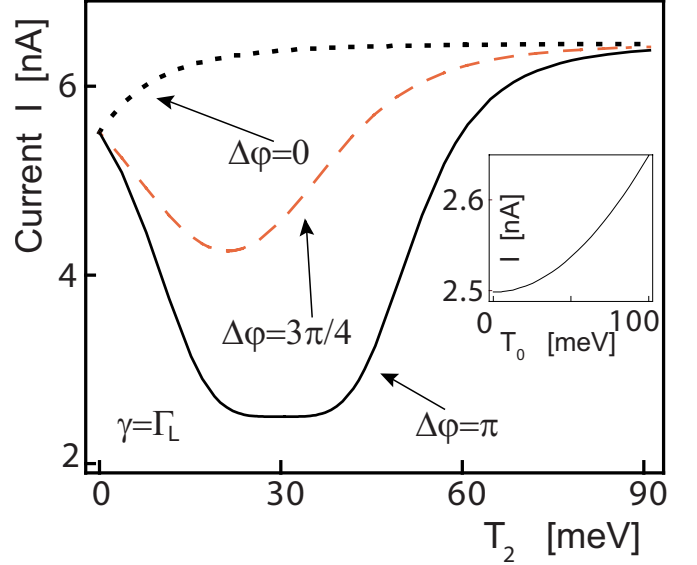


FIG. 2. (Color online) Under the influence of two independent condensates, the dotted, red-dashed, and continuous black curves represent the current through the QD p - i - n junction for different values of phase difference: $\varphi_1 - \varphi_2 = 0, 3\pi/4$, and π , respectively. In plotting the figure, the values of T_1 ($=30$ meV) and incoherent rate γ ($\gamma = \Gamma_L$) are kept fixed. The inset shows the current increases when increasing the condensation number N ($\propto T_0^2$) for the case of only a single condensate. T_0 is the coupling strength between the dot exciton and the cavity photon.

$$H_{2\text{ex-ph}} = \sum_{j=1,2} \{T_j e^{i\varphi_j} |\uparrow\rangle\langle\downarrow| + \sum_{\mathbf{k}} D_{j,\mathbf{k}} |\uparrow\rangle\langle\downarrow| \hat{\beta}_{j,\mathbf{k}}\} + \text{H.c.}, \quad (10)$$

where the two phases φ_1 and φ_2 come from the $U(1)$ symmetry-breaking of the two condensates. Assuming that the exciton-photon couplings of the two wells are identical, the *coherent* parts, $T_j = \sqrt{N_j} D_{\mathbf{k}_0}$, contain the information of the excitation numbers N_1 and N_2 . The resultant steady-state current is similar to Eq. (7), besides the following replacement:

$$T_0^2 \rightarrow D_{\mathbf{k}_0}^2 [N_1 + 2\sqrt{N_1 N_2} \cos(\varphi_1 - \varphi_2) + N_2]. \quad (11)$$

For a fixed N_1 , the dotted, red-dashed, and black curves in Fig. 2 represent the steady-state currents as functions of N_2 , for the phase differences $\varphi_1 - \varphi_2 = 0, 3\pi/4$, and π , respectively. As seen in Fig. 2, the dips in the currents reveal the effect of destructive interference when $\varphi_1 - \varphi_2$ approaches π .

We also suggest that the p - i - n junction can be embedded inside an array of polariton condensates connected by weak periodic potential barriers,⁶ where the in-phase (“zero state”) and antiphase (“ π state”) have been created. In this case, Eqs. (7) and (11) can also be used to distinguish the zero state and π state.

V. SHOT-NOISE MEASUREMENTS

Recently, interest in measurements of shot-noise in quantum transport has grown owing to the possibility of extract-

ing valuable information not available in conventional dc transport experiments.¹⁹ Therefore, in addition to the current, we now proceed to calculate the noise spectrum.

In a quantum conductor out of equilibrium, electronic current-noise originates from the dynamical fluctuations of the current away from its average. To study correlations between carriers, we relate the exciton dynamics with the hole reservoir operators by introducing the degree of freedom n as the number of holes that have tunneled through the barrier connected to the reservoir of holes and write

$$\begin{aligned} \dot{n}_0^{(n)}(t) &= -\Gamma_L n_0^{(n)}(t) + \Gamma_R n_{\downarrow}^{(n-1)}(t), \\ \dot{n}_{\uparrow}^{(n)}(t) &= \Gamma_L n_0^{(n)}(t) + iT[p_{\uparrow,\downarrow}^{(n)}(t) - p_{\downarrow,\uparrow}^{(n)}(t)] - \gamma n_{\uparrow}^{(n)}(t), \\ \dot{n}_{\downarrow}^{(n)}(t) &= -\Gamma_R n_0^{(n)}(t) - iT[p_{\uparrow,\downarrow}^{(n)}(t) - p_{\downarrow,\uparrow}^{(n)}(t)] + \gamma n_{\downarrow}^{(n)}(t), \end{aligned} \quad (12)$$

where $n_j^{(n)}(t)$, $j=0, \uparrow, \downarrow$, represent the time-dependent occupation probabilities for the diagonal elements: $|0\rangle\langle 0|$, $|\uparrow\rangle\langle \uparrow|$, and $|\downarrow\rangle\langle \downarrow|$, respectively. Here, $p_{\uparrow,\downarrow}(t)$ and $p_{\downarrow,\uparrow}(t)$ are the off-diagonal matrix elements: $|\uparrow\rangle\langle \downarrow|$ and $|\downarrow\rangle\langle \uparrow|$. T is the ‘‘coherent’’ interaction that the dot experiences. The superscript ‘‘ n ’’ in $n_j^{(n)}(t)$ refers to the n holes that have tunneled the barrier connecting to the hole reservoir.

Equations (12) allow us to calculate the particle current and the noise spectrum $S_{I_R}(\omega)$ from $P_n(t) = n_0^{(n)}(t) + n_{\uparrow}^{(n)}(t) + n_{\downarrow}^{(n)}(t)$, which gives the total probability of finding n electrons in the collector at time t . In particular, the noise spectrum S_{I_R} can be calculated via the MacDonald formula²⁰

$$S_{I_R}(\omega) = 2\omega e^2 \int_0^{\infty} dt \sin(\omega t) \frac{d}{dt} [\langle n^2(t) \rangle - (\langle n(t) \rangle)^2], \quad (13)$$

where $\frac{d}{dt} \langle n^2(t) \rangle = \sum_n n^2 P_n(t)$. From Eqs. (12) and (13), we obtain

$$S_{I_R}(\omega) = 2eI \{1 + \Gamma_R [\tilde{n}_{\downarrow}(-i\omega) + \tilde{n}_{\downarrow}(i\omega)]\}, \quad (14)$$

where $\tilde{n}_{\downarrow}(z)$ is the Laplace transformation of $n_{\downarrow}(t)$.

By fixing $T_1 = 30$ meV and $\varphi_1 - \varphi_2 = \pi$, an interference effect can be observed in the noise spectrum as a function of T_2 and ω , as shown in Fig. 3(a). The figure shows two symmetric lobes around $T_2 = T_1$, which represent the local minima. To understand these features, we plot in Fig. 3(b) the *Fano factor* (i.e., the *zero-frequency noise* divided by the current) as a function of T_2 for different values of the incoherent decay rate γ . One clearly finds that the magnitude of the central peak decreases when increasing γ . As the incoherent process dominates due to the noncondensate photons overwhelming the coherent ones, the Fano factor reduces to the usual sub-Poissonian limit.²¹ In the opposite limit ($\gamma \rightarrow 0$), the Fano factor approaches unity, i.e., the Poissonian value, demonstrating that the revealing feature of destructive interference is a peak in the Fano factor (at $\omega = 0$), coinciding with the dip in the steady-state current observed in Fig. 2.

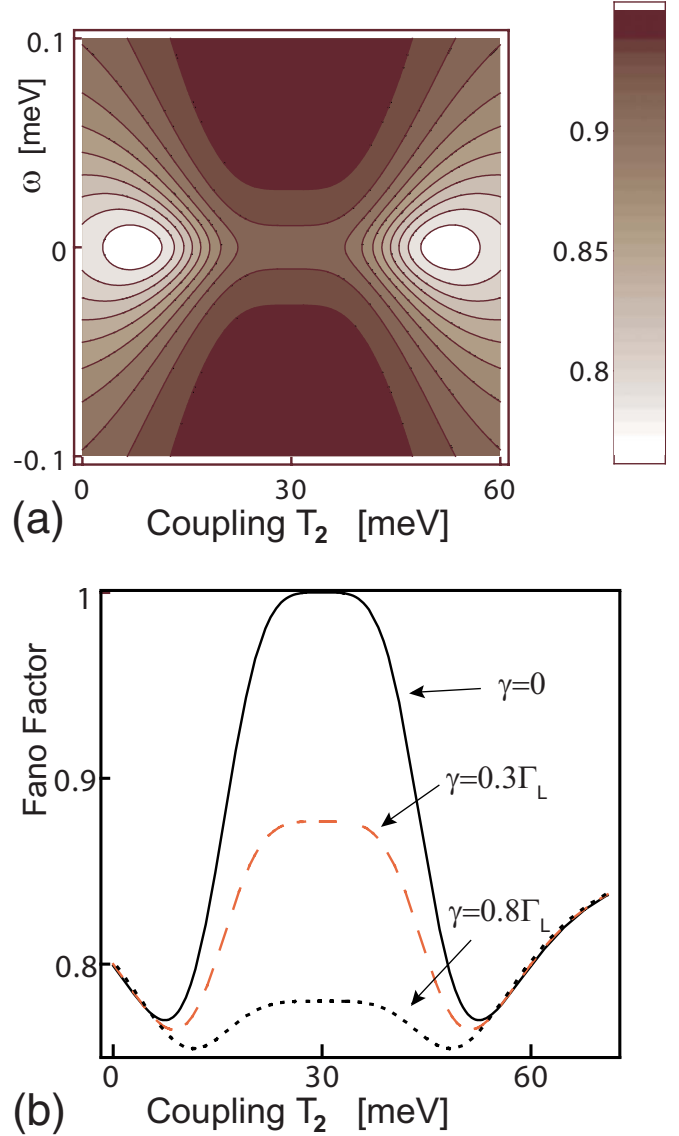


FIG. 3. (Color online) (a) Shot-noise spectra of a QD p - i - n junction as functions of both ω and the coupling T_2 to the second condensate. Here, the excitons are coupled to two condensates. Similar to Fig. 2, one of the condensate numbers is kept fixed, i.e., $T_1 = 30$ meV. (b) By fixing the phase difference $\varphi_1 - \varphi_2 = \pi$, the continuous black, red dashed, and dotted curves represent the Fano factor (zero-frequency noise) for $\gamma = 0$, $0.3\Gamma_L$, and $0.8\Gamma_L$, respectively. The Fano factor is defined here as $S_{I_R}(\omega \rightarrow 0)/2eI$.

VI. CONCLUDING REMARKS

In summary, we have shown that a single QD p - i - n junction can serve as a minidetector²² of a polariton condensate. As the condensation occurs, the two-level exciton couples with the photonic part of condensation polaritons and results in a coherent tunneling inside the dot. The strength of the coherent tunneling increases with the condensation number.

Furthermore, we have also shown that the features of interference can be readout via the electrical current and current-noise if the QD p - i - n junction is coupled to two condensates. Other features of polariton condensation, such as vortex and nonequilibrium behavior, may also be readout by

such a hybrid structure and deserves to be investigated in the near future.

Finally, we mention that an alternative way to detect the condensation of polaritons via electron transport is by directly embedding the quantum well between a p - n junction. We expect that in this case the increase in the steady-state current with the condensation number N might be observable. However, the features we observed in the current-noise spectrum may be invisible since the assumption of three dot states is not valid in a quantum well.

ACKNOWLEDGMENTS

We would like to thank S. A. Gurvitz for helpful discussions. This work is supported partially by the National Science Council of Taiwan under the Grant No. 98-2112-M-006-002-MY3. F.N. acknowledges partial support from the National Security Agency (NSA), Laboratory for Physical Sciences (LPS), Army Research Office (ARO), and National Science Foundation (NSF) under Grant No. EIA-0130383, and JSPS-RFBR under Contract No. 06-02-91200.

*yuehnan@mail.ncku.edu.tw

¹L. D. Landau and E. M. Lifshitz, *Statistical Physics* (Pergamon, London, 1969).

²L. P. Pitaevskii and S. Stringari, *Bose-Einstein Condensation* (Clarendon, Oxford, 2003).

³S. A. Moskalenko, Fiz. Tverd. Tela (Leningrad) **4**, 276 (1962) [Sov. Phys. Solid State **4**, 199 (1962)]; J. M. Blatt, Phys. Rev. **126**, 1691 (1962); L. V. Keldysh and A. N. Kozlov, Zh. Eksp. Teor. Fiz. **54**, 978 (1968) [Sov. Phys. JETP **27**, 521 (1968)].

⁴For a review see, e.g., D. W. Snoke, Phys. Status Solidi B **238**, 389 (2003).

⁵J. Kasprzak, M. Richard, S. Kundermann, A. Baas, P. Jeambrun, J. M. J. Keeling, F. M. Marchetti, M. H. Szymańska, R. André, J. L. Staehli, V. Savona, P. B. Littlewood, B. Deveaud, and Le Si Dang, Nature (London) **443**, 409 (2006).

⁶C. W. Lai, N. Y. Kim, S. Utsunomiya, G. Roumpos, H. Deng, M. D. Fraser, T. Byrnes, P. Recher, N. Kumada, T. Fujisawa, and Y. Yamamoto, Nature (London) **450**, 529 (2007).

⁷K. G. Lagoudakis, M. Wouters, M. Richard, A. Baas, I. Carusotto, R. André, Le Si Dang, and B. Deveaud-Plédran, Nat. Phys. **4**, 706 (2008).

⁸S. Utsunomiya, L. Tian, G. Roumpos, C. W. Lai, N. Kumada, T. Fujisawa, M. Kuwata-Gonokami, A. Löffler, S. Hoffling, A. Forchel, and Y. Yamamoto, Nat. Phys. **4**, 700 (2008).

⁹A. Amo, D. Sanvitto, F. P. Laussy, D. Ballarini, E. del Valle, M. D. Martin, A. Lemaître, J. Bloch, D. N. Krizhanovskii, M. S. Skolnick, C. Tejedor, and L. Vina, Nature (London) **457**, 291 (2009).

¹⁰C. Cohen-Tannoudji, J. Dupont-Roc, and G. Grynberg, *Atom-Photon Interactions: Basic Processes and Applications* (Wiley-VCH, New York, 1992).

¹¹J. P. Reithmaier, G. Sek, A. Löffler, C. Hofmann, S. Kuhn, S. Reitzenstein, L. V. Keldysh, V. D. Kulakovskii, T. L. Reinecke, and A. Forchel, Nature (London) **432**, 197 (2004); E. Peter, P. Senellart, D. Martrou, A. Lemaître, J. Hours, J. M. Gérard, and J. Bloch, Phys. Rev. Lett. **95**, 067401 (2005).

¹²T. Yoshie, A. Scherer, J. Hendrickson, G. Khitrova, H. M. Gibbs, G. Rupper, C. Ell, O. B. Shchekin, and D. G. Deppe, Nature (London) **432**, 200 (2004); K. Hennessy, A. Badolato, M. Winger, D. Gerace, M. Atature, S. Gulde, S. Falt, E. L. Hu, and A. Imamoglu, *ibid.* **445**, 896 (2007).

¹³Z. Yuan, B. E. Kardynal, R. M. Stevenson, A. J. Shields, C. J. Lobo, K. Cooper, N. S. Beattie, D. A. Ritchie, and M. Pepper, Science **295**, 102 (2002).

¹⁴See, e.g., Y. N. Chen, D. S. Chuu, and T. Brandes, Phys. Rev. Lett. **90**, 166802 (2003).

¹⁵S. A. Moskalenko and D. W. Snoke, *Bose-Einstein Condensation of Excitons and Biexcitons* (Cambridge University Press, Cambridge, England, 2000).

¹⁶R. Aguado and T. Brandes, Phys. Rev. Lett. **92**, 206601 (2004); N. Lambert and F. Nori, Phys. Rev. B **78**, 214302 (2008).

¹⁷Y. N. Chen and D. S. Chuu, Phys. Rev. B **66**, 165316 (2002).

¹⁸M. R. Andrews, C. G. Townsend, H.-J. Miesner, D. S. Durfee, D. M. Kurn, and W. Ketterle, Science **275**, 637 (1997).

¹⁹See, e.g., C. W. J. Beenakker, Rev. Mod. Phys. **69**, 731 (1997); Y. M. Blanter and M. Buttiker, Phys. Rep. **336**, 1 (2000).

²⁰D. K. C. MacDonald, Rep. Prog. Phys. **12**, 56 (1949).

²¹Y. N. Chen, T. Brandes, C. M. Li, and D. S. Chuu, Phys. Rev. B **69**, 245323 (2004).

²²P. Neutens, P. V. Dorpe, I. D. Vlamincck, L. Lagae, and G. Borghs, Nat. Photonics **3**, 283 (2009).